Available online at www.sciencedirect.com
SCIENCE DIRECT®
International Journal of Mass Spectrometry 228 (2003) 1035–1054
International Journal of Mass Spectrometry
www.elsevier.com/locate/ijms

Application of the kinetic method to bifunctional bases ESI tandem quadrupole experiments

Guy Bouchoux*, David-Alexandre Buisson, Sophie Bourcier, Michel Sablier

Laboratoire des Mécanismes Réactionnels, Ecole Polytechnique, UMR CNRS 7651, DCMR, F-91128 Palaiseau Cedex, France

Received 18 November 2002; accepted 28 April 2003

Abstract

The applicability of the kinetic method to the determination of the basicity of bidentate molecules has been assessed by considering several molecules M previously studied by equilibrium method (M = acetone (**1**), 1,3-propanediol (**2**), glycerol (**3**), 1,4-butanediol (**4**), 1,3-propanolamine (**5**), 1,4-butanolamine (**6**), 1,3-propanediamine (**7**) and 1,4-butanediamine (**8**)). Protonated adducts $[MHB_i]^+$ (where B_i is a reference base) were produced by electrospray ionisation and analysed by tandem quadrupole mass spectrometry. Application of the classical correlation of the natural logarithm of the ratio of peak intensities, $\ln([MH]^+/[B_iH]^+)$, with either the proton affinities (PA) or the gas phase basicities (GB) of the reference bases B_i to deduce PA(M) or GB(M) has been examined. It is confirmed that only the use of several experiments at different collision energies ("extended" or "isothermal point" methods) may lead to meaningful results. Good agreement is observed between the PA(M) values tabulated or obtained from the isothermal point for molecule M = **1** and **5**–**8**. However, the present PA values appear to be different from that obtained by equilibrium method in the case of diols **2**–**4**. It is generally observed that the measured "apparent" protonation entropies of all the bifunctional molecules examined are significantly less than that obtained by equilibrium methods.

Keywords: Kinetic method; Bidentate bases; Proton affinity; Gas phase basicity; Protonation entropy

1. Introduction

The "kinetic method" has been used to estimate thermochemical data for a wide range of organic molecules for more than 20 years (for recent reviews on the kinetic method see [1]). Basically, it consists in relating the ratio of the peak intensities associated with two competitive dissociation channels to a difference in thermochemical properties of the corresponding products. For example, the dissociation of the proton-bound dimer $[MHB_i]^+$ (Scheme 1) may lead to the differences in gas phase basicities, GB, or proton affinities, PA, of M and B_i through the ratio of peak intensities $[MH]^+/[B_iH]^+$. The desired quantitative relationship and the significance of the data are however dependent upon a number of assumptions. Recently, critical discussions have been raised concerning the validity of the results given by the kinetic method when entropy effects have to be considered in the data analysis [2–6]. Surprisingly enough, no systematic experimental study on well-defined systems has been undertaken in order to tackle this question

* Corresponding author. Tel.: +33-1-69-33-34-00; fax: +33-1-69-33-30-10.
E-mail address: bouchoux@dcmr.polytechnique.fr (G. Bouchoux).

1387-3806/$ – see front matter © 2003 Elsevier Science B.V. All rights reserved.
doi:10.1016/S1387-3806(03)00219-7

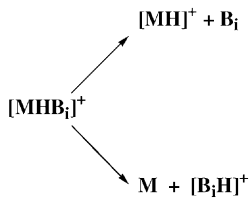

Scheme 1.

until a recent past. Accordingly, a study in the laboratory, involving MIKE and CID–MIKE experiments, shows that the application of the kinetic method to species M associated with important entropy changes upon protonation leads to results at variance from previous estimates based on proton transfer equilibrium constant measurements [6]. The goal of the present study is to further examine these situations when experiments are conducted on a tandem quadrupole mass spectrometer, an apparatus which has been widely used to obtain thermochemical information by the kinetic method.

With the exception of acetone (**1**), the studied molecules (1,3-propanediol (**2**), glycerol (**3**), 1,4-butanediol (**4**), 1,3-propanolamine (**5**), 1,4-butanolamine (**6**), 1,3-propanediamine (**7**), 1,4-butanediamine (**8**)) present two remote basic sites, a situation which is expected to produce a strongly chelated protonated form and to consequently induce an increase in proton affinity and a significant entropy change. Accordingly, these molecules have been previously studied by equilibrium methods at various temperatures and their proton affinities and entropy of protonation (defined as $\Delta_p S^\circ(\mathrm{M}) = S^\circ([\mathrm{MH}]^+) - S^\circ(\mathrm{M})$) have been deduced from the corresponding van't Hoff plots [7–12]. Indeed, negative values of $\Delta_p S^\circ(\mathrm{M})$ have been reported for **2**–**8**, demonstrating for these molecules an efficient entropy loss resulting from the decrease of freedom when passing from the neutral molecule to its protonated form.

The applicability of the kinetic method to the determination of the basicity properties of molecules **2**–**8** has been tested here by using a tandem quadrupole mass spectrometer, proton bound heterodimers were produced in an electrospray source.

2. Experimental

ES–MS and collision-induced dissociation (CID) MS/MS was carried out on a Micromass (Manchester, UK) tandem quadrupole (QhQ, where Q and h stand for quadrupole and hexapole, respectively) Quattro II mass spectrometer equipped with an electrospray ion source. Cone voltage was set to the lowest value compatible with a good compromise between sensibility of detection and high yield of the protonated dimer, the value of 5 V has been retained throughout this study. The capillary voltage was varied between 3.0 and 3.5 kV to optimise the conditions for obtaining maximum intensity of the protonated dimers. Typical values for the other source parameters were: counter electrode 0.5 kV, rf lens 0.2 V, skimmer 1.2 V, skimmer lens offset 5 V and source temperature 80 °C.

The ions of interest were selected in the first quadrupole and activated by collision in the rf-only hexapole using argon as the collision gas at a pressure of 1.5–2 $\times$ 10^{-3} mbar. The dissociation products were mass analysed by scanning the second quadrupole of the QhQ device. Experimental data have been collected at several different collision energies in the laboratory frame, E_{lab}, situated between 0 and 24 V. The centre of mass collision energy has been calculated by the usual conversion expression: $E_{\mathrm{cm}} = E_{\mathrm{lab}} \cdot m_{\mathrm{target}}/(m_{\mathrm{target}} + m_{\mathrm{ion}})$. A scan rate of 1 s scan^{-1} was used for both experiments with a data acquisition duration of 1 min for each energy step and a *m*/*z* scanning range of 30–250 u. The acquired spectra were summed for interpretation.

Sample solutions were prepared in methanol and dissolved to achieve typically a concentration of 10^{-4} M. All solutions were infused at a flow rate of 10^{-2} mL min^{-1} with a Harvard Apparatus syringe pump (Southmatic, MA, USA). The samples, bases and solvents of HPLC grade were purchased from Sigma–Aldrich (St. Quentin Fallavier, France) and used as received without any further purification.

GB and PA values of the reference bases B_i were coming from the Hunter and Lias compilation [12] unless otherwise specified.

3. Results and discussion

3.1. Experimental results

For each molecule M = **1**–**8**, a series of reference bases B_i has been used to produce the relevant proton bound dimer $[MHB_i]^+$ (for the details on these experiments, see Tables A.1–A.8 and Figs. A.1–A.8 in Appendix A). The CIDs of $[MHB_i]^+$ were examined by the "kinetic method", i.e., the natural logarithm of the ratio of the fragment ion abundances $y_i = \ln([MH]^+/[B_iH]^+)$ has been correlated with the gas phase basicities $GB(B_i)$ or the proton affinities $PA(B_i)$ of the reference bases B_i. Each y_i versus $GB(B_i)$ or $PA(B_i)$ plot has been treated by a linear curve fitting procedure.

One advantage of the tandem quadrupole device is the possibility to control the kinetic energy of the selected protonated dimer $[MHB_i]^+$ before it enters into collision with the target gas. A typical example is presented in Fig. 1 where the intensities of the fragment ions *m/z* 75 (protonated 1,3-diaminopropane) and *m/z* 88 (protonated diethylmethyl amine) coming from dissociations of the mass selected precursor *m/z* 162 (protonated 1,3-diaminopropane/diethylmethyl amine adduct) are plotted as a function of the centre of mass collision energy, E_{cm}. At high collision energies, since secondary fragmentations occur, the intensities of the $[MH]^+$ and $[B_iH]^+$ ions and their fragment were summed before evaluating y_i.

From these data the $\ln([MH]^+/[B_iH]^+)$ versus E_{cm} curve may be traced. A linear relationship is generally observed in a large part of the collision energy range as illustrated in Fig. 1. Note that $E_{cm} = 0$ eV is above but close to the onset of the fragment ions. E_{cm} is thus not, strictly speaking, the "centre of mass collision energy" but rather a "centre of mass excess energy", i.e., the maximum excess energy imparted by the collision to the dissociating protonated dimer. Extrapolation to $E_{cm} = 0$ eV is expected to correspond to species spontaneously dissociating in the rf-only hexapole (i.e., the "metastable ions"). The results discussed below correspond to $y_i = \ln([MH]^+/[B_iH]^+)$ values determined, via the linear fitting of the curves of the type presented in Fig. 1b, at $E_{cm} = 0$, 2 and 4 eV. These experimental data together with relevant thermochemical parameters ($GB(B_i)$, $PA(B_i)$ and $\Delta_p S^\circ_{298}(B_i)$) are given in Appendix A, the major results are summarised in Tables 1 and 2. They will be discussed after a brief recall of the classical thermochemical approach of the kinetic method, including the consideration of the entropy effects.

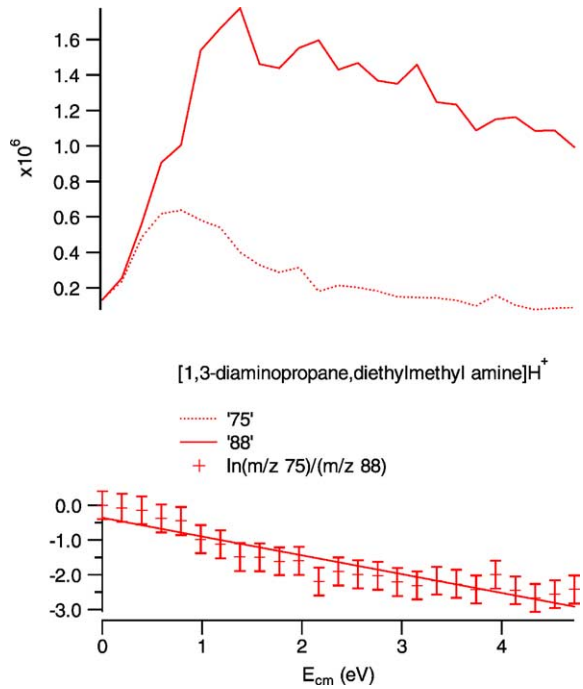

Fig. 1. Typical representative curve of the fragment ions abundance as a function of the centre of mass collision energy. Dissociation of the proton bound dimer of 1,3-diaminopropane and diethylmethyl amine. Upper traces, *m/z* 75 and 88 fragment ion abundance; lower trace natural logarithm of the abundance ratio and linear curve fitting.

3.2. Basic equations

As it is classical in applying the kinetic method to the competitive process depicted in Scheme 1, it is first assumed that the product ion abundance reflect the corresponding rate constants, one may thus write:

$$y_i = \ln\left(\frac{[MH]^+}{[B_iH]^+}\right) = \ln\frac{k_{MH}}{k_{B_iH}}$$

Table 1
Summary of the proton affinities and gas phase basicities data for molecules **1**–**8**

M	Proton affinity (kJ mol^{-1})				Gas phase basicity (kJ mol^{-1})				
	PA_{298} (lit)[a]	PA_{app} (obs.)[b]	PA (Eq. (2a′))	PA_{iso}[c]	GB_{298} (lit)[a]	GB_{app} (obs.)[b]	GB (Eq. (2b′))	GB_{iso}[c]	GB (Eq. (3b′))
1, Acetone	812.0	815.2	814.3	812.6 ± 0.2 [812.4 ± 0.1]	782.1	784.7	782.2	782.0 ± 0.2	779.7
		815.9	814.9			785.4	782.6		
		817.2	815.8			786.8	783.6		
2, 1,3-Propanediol	876.2	850.4	837.9	857.6 ± 0.5 [858.3 ± 0.8]	825.9	820.0	808.0	827.3 ± 0.2	846.3
		848.5	827.6			818.1	797.7		
		845.2	810.3			814.7	780.3		
3, Glycerol	874.8	840.7	835.8	848.6 ± 1.2 [848.2 ± 1.6]	820.0	810.2	805.5	818.9 ± 0.5	844.5
		838.7	819.7			807.9	789.4		
		835.4	796.3			804.1	766.0		
4, 1,4-Butanediol	915.6	875.0	871.7	884.3 ± 0.5 [883.3 ± 0.1]	855.0	843.5	841.2	852.9 ± 0.5	885.2
		872.7	860.1			841.1	829.7		
		868.4	840.2			836.8	809.8		
5, 1,3-Propanolamine	962.5	945.3	936.0	953.5 ± 1.6 [953.8 ± 0.3]	917.3	912.5	903.8	921.3 ± 1.2	929.4
		943.4	933.2			910.5	901.0		
		940.5	929.5			907.4	897.4		
6, 1,4-Butanolamine	984.5	961.1	955.5	971.9 ± 0.2 [971.9 ± 0.1]	932.1	928.5	920.6	939.4 ± 0.2	951.6
		956.4	947.5			923.8	912.3		
		944.6	933.7			911.8	898.0		
7, 1,3-Propanediamine	987.0	971.0	966.3	981.2 ± 1.4 [981.1 ± 0.3]	940.0	939.4	932.9	949.6 ± 1.7	955.5
		966.6	960.5			935.1	926.9		
		958.7	952.0			927.4	917.5		
8, 1,4-Butanediamine	1005.6	982.3	977.4	991.6 ± 0.2 [991.8 ± 0.9]	954.3	951.1	944.5	960.8 ± 0.2	974.3
		978.5	969.8			947.2	937.1		
		969.4	956.5			937.8	924.9		

[a] From ref. [12].
[b] Intercept of the correlation line with the *x*-axis.
[c] *x* co-ordinate of the isothermal point. Into bracket, values obtained by using the $\ln([MH]^+/[B_iH]^+) + \Delta_p S^\circ(B_i)$ vs. $PA_{298}(B_i)$ plot.

Table 2
Summary of the entropy contributions associated with protonation of molecules **1**–**8** ($J^1\,mol^{-1}\,K^-$)

M	$\Delta_pS^\circ(M)_{lit}$	$\Delta_pS^\circ(B_i)_{average}$ [a]	ΔS° [b]	ΔS°_{iso} [c]	$\Delta_pS^\circ(M)_{iso}$
1, Acetone	15.8 ± 7.2[d]	6.3 ± 1.4	9.5 ± 8.6	8.4 ± 0.5	14.7 ± 1.9
2, 1,3-Propanediol	−61.8 ± 4.3[e]	6.6 ± 2.6	−68.4 ± 6.9	−12.9 ± 1.0	−6.3 ± 3.6
3, Glycerol	−75[f]	6.6 ± 3.9	−81.6 ± 3.9	−21.2 ± 0.9	−14.6 ± 4.8
4, 1,4-Butanediol	−97.2 ± 5.9[e]	3.4 ± 1.8	−100.6 ± 7.7	−21.0 ± 1.5	−17.6 ± 3.3
5, 1,3-Propanolamine	−43[g]	−2.3 ± 3.7	−40.7 ± 3.7	−19.3 ± 2.1	−21.6 ± 5.8
6, 1,4-Butanolamine	−67[g]	−0.8 ± 4.0	−65.3 ± 4.3	−25.3 ± 1.0	−26.1 ± 5.3
7, 1,3-Propanediamine	−49[g] (−86[h])	3.1 ± 3.9	−52.1 ± 3.9	−31.0 ± 2.7	−27.9 ± 6.6
8, 1,4-Butanediamine	−63[g]	4.1 ± 3.4	−67.1 ± 3.4	−19.1 ± 1.1	−15.0 ± 4.5

[a] Mean value of the $\Delta_pS^\circ(B_i)$ quoted in ref. [12], indicated errors are standard deviations. For details see Tables A.1–A.8.
[b] Defined as $\Delta S^\circ = \Delta_pS^\circ(M) - \Delta_pS^\circ(B_i)_{average}$ and calculated using the literature values given in columns 2 and 3.
[c] Deduced from isothermal points using Eq. (3c′): $\Delta S^\circ_{iso} = y_{iso}/R$ ($R = 8.3145\,J\,mol^{-1}\,K^{-1}$).
[d] Mean value from refs. [15–18].
[e] From ref. [7].
[f] From ref. [8].
[g] From ref. [9].
[h] From ref. [11].

If the decomposing species $[MHB_i]^+$ are considered to be at thermal equilibrium at a temperature T, application of the transition state theory leads to:

$$y_i = \ln\left(\frac{[MH]^+}{[B_iH]^+}\right) = \ln\frac{k_{MH}}{k_{B_iH}} = \frac{-\Delta G_i^\ddagger}{RT} \quad (1)$$

where $\Delta G_i^\ddagger$ is the Gibbs free energy difference between the two transition structures TS($[MH]^+$) and TS($[B_iH]^+$) associated with reactions $[MHB_i]^+ \rightarrow B_i + [MH]^+$ and $[MHB_i]^+ \rightarrow [B_iH]^+ + M$, respectively. When expressing the free energy difference $\Delta G_i^\ddagger$ in terms of proton affinities of M and B_i and introducing the difference in reverse activation enthalpies $\Delta_R H_i^\ddagger = \Delta_R H^\ddagger([MH]^+) - \Delta_R H^\ddagger([B_iH]^+)$ [$\Delta_R H^\ddagger([MH]^+) = H^\circ$(transition structure TS($[MH]^+$)) − $H^\circ(B_i + [MH]^+)$ and $\Delta_R H^\ddagger([B_iH]^+) = H^\circ$(transition structure TS($[B_iH]^+$)) − $H^\circ(M + [B_iH]^+)$], Eq. (1) should write [6]:

$$y_i = \frac{1}{RT}[PA_{298}(M) - PA_{298}(B_i) - \Delta_R H_i^\ddagger + T\,\Delta S_i^\ddagger] \quad (1a)$$

Similarly, using the gas phase basicities:

$$y_i = \frac{1}{RT}[GB_{298}(M) - GB_{298}(B_i) - \Delta_R H_i^\ddagger + T\,\Delta S_i^\ddagger - 298\,\Delta S_i^\circ] \quad (1b)$$

where $\Delta S_i^\circ = \Delta_pS^\circ(M) - \Delta_pS^\circ(B_i)$ ($\Delta_pS^\circ(X) = S^\circ([XH]^+) - S^\circ(X)$).

Under these assumptions, the correlation lines:

$$y_i = a[PA_{app}(M) - PA_{298}(B_i)] \quad (1a')$$

$$y_i = b[GB_{app}(M) - GB_{298}(B_i)] \quad (1b')$$

would have a common slope $a = b = 1/RT$, and an x-axis intercept at:

$$PA_{app}(M) = PA_{298}(M) - \Delta_R H^\ddagger + T\,\Delta S^\ddagger \quad (2a)$$

$$GB_{app}(M) = GB_{298}(M) - \Delta_R H^\ddagger + T\,\Delta S^\ddagger - 298\,\Delta S^\circ \quad (2b)$$

where all the parameters relevant to the set of reference bases B_i have to be averaged (i.e., $\Delta_R H^\ddagger = \langle\Delta_R H_i^\ddagger\rangle$, $\Delta S^\ddagger = \langle\Delta S_i^\ddagger\rangle$ and $\Delta S^\circ = \langle\Delta S_i^\circ\rangle$).

The usual approximation [1] consists to consider that $\Delta G_i^\ddagger \sim \Delta G_i^\circ$ (i.e., $\Delta_R H_i^\ddagger$ is negligible and that $\Delta S_i^\ddagger \sim \Delta S_i^\circ$) and consequently Eqs. (2a) and (2b) reduce to:

$$PA_{app}(M) = PA_{298}(M) + T\,\Delta S^\circ \quad (2a')$$

$$GB_{app}(M) = GB_{298}(M) + (T - 298)\,\Delta S^\circ \quad (2b')$$

In order to remove the uncertainties due to averaging the ΔS° it is obviously convenient, as far as

possible, to select bases B_i with comparable $\Delta_p S^\circ(B_i)$ (thus not necessarily bases pertaining to the same chemical class). It is also possible to take explicitly into account each individual $\Delta_p S^\circ(B_i)$ by defining a new variable y'_i such as $y'_i = y_i + \Delta_p S^\circ(B_i)/R$ [2e]. Under these circumstances, the *x*-axis intercept of the plots y'_i versus $PA_{298}(B_i)$ or $GB_{298}(B_i)$ becomes:

$$PA'_{app}(M) = PA_{298}(M) + T\,\Delta_p S^\circ(M) \quad (2a'')$$

$$GB'_{app}(M) = GB_{298}(M) + (T - 298)\,\Delta_p S^\circ(M) \quad (2b'')$$

Note, however, that most of the time the tabulated $\Delta_p S^\circ(B_i)$ are estimated by comparison with values measured for similar compounds. The error inherent to these assignments is not easy to appreciate but it cannot be ignored. It is sufficient to observe that an uncertainty of $8\,J\,mol^{-1}\,K^{-1}$ on $\Delta_p S^\circ(B_i)$ introduces an error of one unit on y'!

3.3. Use of the "isothermal" point

If several experiments at various temperatures *T* are available, it is theoretically possible to deduce both $PA_{298}(M)$ and ΔS°, and thus $\Delta_p S(M)$, from Eq. (2a′) by a van't Hoff like treatment. This approach (the so-called "extended kinetic method" or "full entropy analysis") has been extensively used in the last years (the first tentatives of entropy determination by the kinetic method were described in ref. [3]). The usual procedure consists in plotting $PA_{app}(M)/RT$ versus $1/RT$. From examination of Eq. (2a′), it appears that the slope of the plot is $PA_{298}(M)$ and the y intercept equals $\Delta S^\circ/R$. A better statistical approach, using a plot of $(PA_{app}(M) - PA_{average}(B_i))/RT$ versus $1/RT$ (where $PA_{average}(B_i)$ is the mean value of the $PA_{298}(B_i)$'s), has been proposed by Armentrout [2b] in order to remove cross correlation effects. As noted by the same author, another way to obtain $PA_{298}(M)$ and ΔS° is simply to plot $PA_{app}(M)$ versus *T* (see Fig. 6 in ref. [2b] and Fig. 2b here). This is exactly what is suggested by the relationship of Eq. (2a′).

These various procedures needs two graphical treatments: (i) the plots leading to the couples $PA_{app}(M)$ and *T* and (ii) the plot of $PA_{app}(M)/RT$ versus $1/RT$ or $PA_{app}(M)$ versus *T*. In fact, as recently intuitively suggested [4c] and established in more details [6], $PA_{298}(M)$ and ΔS° may be directly deduced from the first plots. Accordingly, the co-ordinates of the point of intercept of the various correlation lines $y_i = f(PA_{298}(B_i))$ (or $y_i = f(GB_{298}(B_i))$), i.e., the "isothermal point", are directly related to $PA_{298}(M)$ (or $GB_{298}(M)$) and ΔS°. It follows from Eqs. (1a) and (1b) that:

$$PA_{iso}(M) = PA_{298}(M) - \Delta_R H^{\ddagger} \quad (3a)$$

$$GB_{iso}(M) = GB_{298}(M) - \Delta_R H^{\ddagger} - 298\,\Delta S^\circ \quad (3b)$$

$$y_{iso} = \frac{\Delta S^{\ddagger}}{R} \quad (3c)$$

And, if the approximation $\Delta G_i^{\ddagger} \sim \Delta G_i^{\circ}$ holds, the preceding equations reduce to:

$$PA_{iso}(M) = PA_{298}(M) \quad (3a')$$

$$GB_{iso}(M) = GB_{298}(M) - 298\,\Delta S^\circ \quad (3b')$$

$$y_{iso} = \frac{\Delta S^\circ}{R} \quad (3c')$$

Again, if a plot of $y'_i = y_i + \Delta_p S^\circ(B_i)/R$ versus $PA_{298}(B_i)$ or $GB_{298}(B_i)$ has been used, then the co-ordinates of the isothermal point are:

$$PA'_{iso}(M) = PA_{298}(M) \quad (3a'')$$

$$GB'_{iso}(M) = GB_{298}(M) - 298\,\Delta_p S^\circ(M) \quad (3b'')$$

$$y'_{iso} = \frac{\Delta_p S^\circ(M)}{R} \quad (3c'')$$

The equivalency of the "extended method" plot and the "isothermal" treatment is illustrated in Fig. 2. For several experiments involving a series of couples M and B_i at various internal energies, effective temperatures T_a, T_b, T_c, etc. are deduced from the slope of the correlation lines $y_i = f(PA_{298}(B_i))$ (Fig. 2(I)). For each effective temperature the intercept of the regression line with the *x*-axis leads to a value of $PA_{app}(M)$ (Eq. (1a′)). To deduce $PA_{298}(M)$ and ΔS° the extended method treatment implies a plot of $PA_{app}(M)$ versus *T*, as presented in Fig. 2(II). In fact it is clear that the

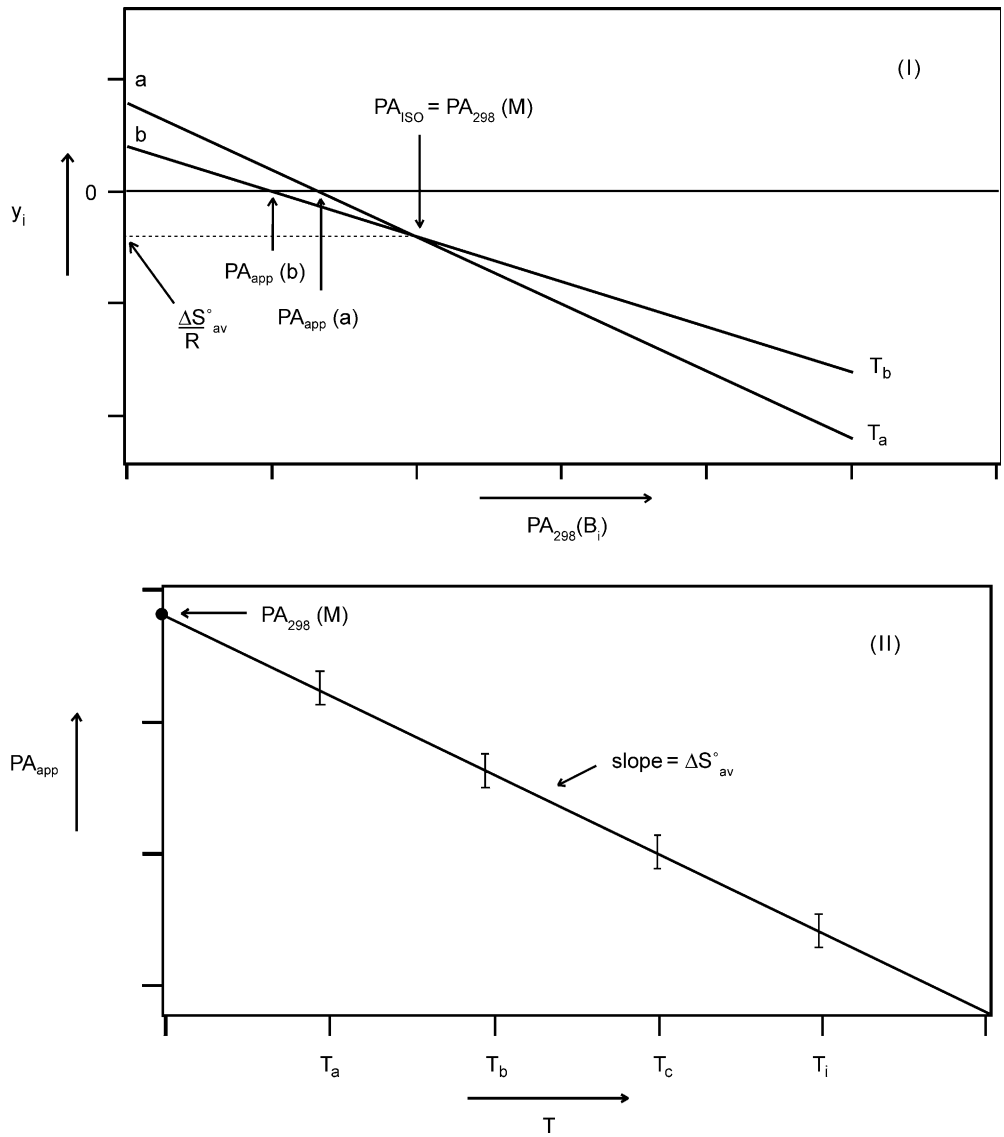

Fig. 2. Idealised diagram of the two plots used in the full entropy analysis method. Plot I: $\ln([MH]^+/[B_iH]^+)$ vs. $PA(B_i)$; plot II: $PA_{app}(M)$ vs. the effective temperature T. The co-ordinates of the isothermal point (plot I) allow directly the determination of $PA_{iso}(M)$ and ΔS°_{iso}.

same information is directly obtained from Fig. 2(I) by considering the co-ordinates of the isothermal point (Eqs. (3a′) and (3c′)).

Application of the isothermal point technique to the determination of $PA_{298}(M)$ and ΔS° for the set of molecules M = **1**–**8** will be discussed in the following section.

3.4. Comparison between experiment and theory

- Before discussing the results given by the kinetic method, the predictions given by the parent Eqs. (2a′) and (2b′) must be examined. Table 1 compares the $PA_{app}(M)$ and $GB_{app}(M)$ experimentally determined for **1**–**8** (i.e., the intercept of the

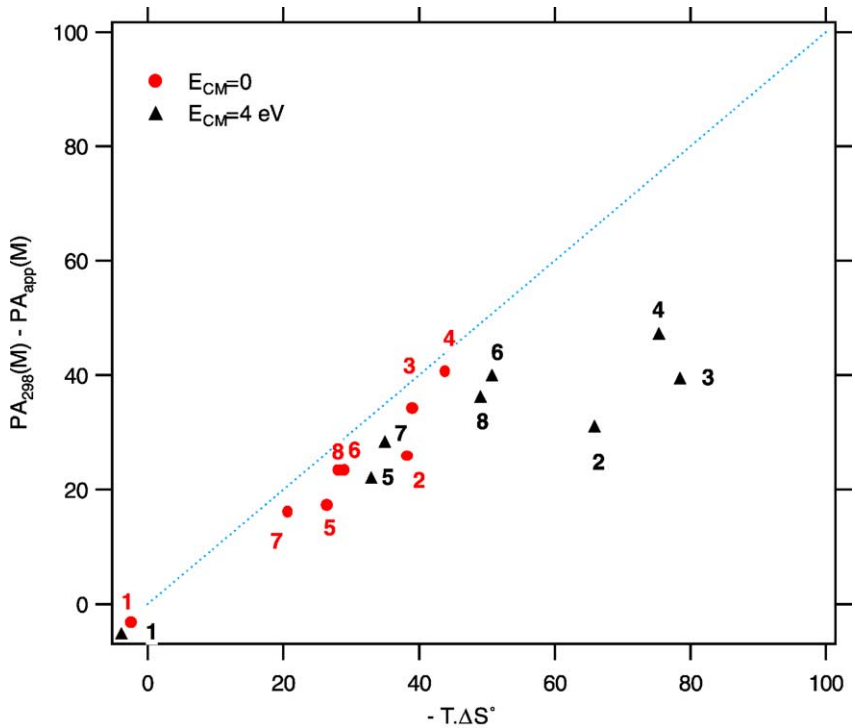

Fig. 3. Observed difference $PA_{298}(M) - PA_{app}(M)$ compared to its theoretical value $-T\,\Delta S^{\circ}$ (Eq. (2a′)).

$y_i = f(PA_{298}(B_i))$ or $y_i = f(GB_{298}(B_i))$ plots with the x-axis) to the results given by Eqs. (2a′) and (2b′). The results obtained at three centre of mass collision energies, $E_{cm} = 0$, 2 and 4 eV, are presented for each molecule M. Figs. 3 and 4 illustrate these comparisons for $E_{cm} = 0$ and 4 eV.

It appears from Table 1 that, for acetone (**1**), the agreement between experimentally determined $PA_{app}(M)$ and $GB_{app}(M)$ and their values deduced from Eqs. (2a′) and (2b′) is reasonable (i.e., the deviation is less than 5 kJ mol^{-1}) whatever the collision energy is. For the molecules **2**–**8**, the deviation is situated in a limited range 0–12 kJ mol^{-1} when the data are obtained under low collisional energy ($E_{cm} = 0$ eV, Table 1). By contrast, the deviation increases with increasing the collision energy to attain ca. 40 kJ mol^{-1} when $E_{cm} = 4$ eV. This is best shown in Fig. 3 where the difference between $PA_{298}(M)$ and the experimental point of intercept $PA_{app}(M)$ is plotted against its theoretical value deduced from Eq. (2a′), i.e., $PA_{298}(M) - PA_{app}(M) = -T\,\Delta S^{\circ}_{average}$. It is clear that the points corresponding to $E_{cm} = 0$ eV are close to the line of unit slope. By contrast, the points relevant to $E_{cm} = 4$ eV are shifted to the right, particularly for the diols **2**–**4**. A comparable observation is made in Fig. 4 where $GB_{298}(M) - GB_{app}(M)$ is plotted against its theoretical value: $-(T - 298)\,\Delta S^{\circ}$ (see Eq. (2b′)).

In fact, in all the cases, the experimental value of the apparent proton affinity, $PA_{app}(M)$, or gas phase basicity, $GB_{app}(M)$, is higher than the value given by Eqs. (2a′) and (2b′), and the discrepancy increases with increasing the collision energy (i.e., the temperature T). This means that the corrective action of the $T\,\Delta S^{\circ}$ term in Eqs. (2a′) and (2b′) is overestimated when using the experimental effective temperature T and the ΔS° difference estimated from the literature data. This conclusion parallels that made using MIKE and CID/MIKE data for the diols **2**–**4**, diamines **7**, **8** and other bidentate bases

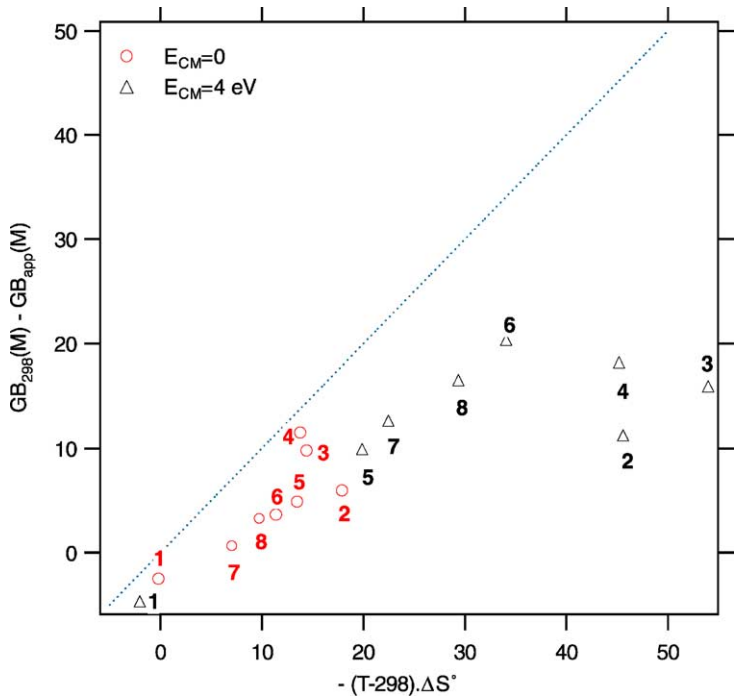

Fig. 4. Observed difference $GB_{298}(M) - GB_{app}(M)$ compared to its theoretical value $-(T - 298)\,\Delta S^{\circ}$ (Eq. (2b′)).

[6]. These observations are confirmed by considering the results given by the isothermal point method, as discussed below.

- Experimental values of $PA_{iso}(M)$ and $GB_{iso}(M)$, given by the isothermal point method, are given in Table 1. In Table 2, the experimental entropy term deduced from Eq. (3c′) is called ΔS°_{iso} and compared with its value expected from the literature data, ΔS°. The corresponding protonation entropies $\Delta_p S^{\circ}(M)_{iso}$ and $\Delta_p S^{\circ}(M)_{lit}$ are also indicated.

Considering first the proton affinity, Fig. 5 shows an excellent agreement between $PA_{iso}(M)$ and its theoretical value $PA_{298}(M)$, for **1**. The agreement is only moderately good for 1,3-propanolamine (**5**), 1,4-butanolamine (**6**), and diamines **7**, **8**. For these four compounds, the mean deviation is ca. 10 kJ mol^{-1}, with a maximum of 14 kJ mol^{-1} for **8**. It is clear from Table 1 and Fig. 5 that the situation is even less comfortable for the diols **2**–**4**. For these three compounds, the experimental proton affinities $PA_{iso}(M)$ differ from $PA_{298}(M)$ by 18.6, 26.2 and 31.3 kJ mol^{-1}, respectively. It is also noteworthy that, systematically, the experimental $PA_{iso}(M)$ value is lower than its true value, $PA_{298}(M)$.

The use of the variable y'_i rather than y_i has a negligible effect on the $PA_{iso}(M)$ values (into brackets, Table 1), the deviation between the two modes of estimate does not exceed 1 kJ mol^{-1} (i.e., is less than the sum of the standard deviations and far from the possible error on the absolute PA(M) values).

Concerning now the entropy term, Table 2 and Fig. 6 illustrate the comparison between the experimental protonation entropy $\Delta_p S^{\circ}(M)_{iso}$ obtained by using the co-ordinate of the isothermal point (Eq. (3c′)) and the corresponding literature value (thus determined by the equilibrium method) $\Delta_p S^{\circ}(M)_{lit}$. The tabulated $\Delta_p S^{\circ}(M)_{lit}$ values were all determined by the equilibrium method at variable temperature and derived from the intercept of van't Hoff plots over a limited temperature range. Deviation of up to 15 J mol^{-1} K^{-1} have been observed for $\Delta_p S^{\circ}$ of simple, monodentate, bases

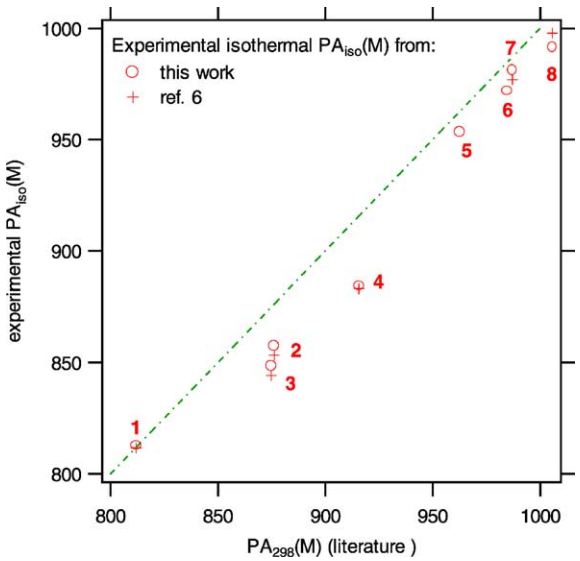

Fig. 5. PA(M) deduced from the isothermal point (Eq. (3a′)) compared to its literature value (ref. [12]).

(such as acetone, isobutene, toluene, methyl formate or *i*-propylcyanide) measured from different laboratories [18]. Similar deviation may be expected for aminoalcohols **5**, **6** and diamines **7**, **8** as suggested by entropy calculations taking into account the hindered internal rotations in both the molecule and their protonated forms [13,14]. Unless clearly specified in the original reference (see Table 2), an uncertainty of $\pm 15\,\mathrm{J\,mol^{-1}\,K^{-1}}$ as been supposed on $\Delta_p S^\circ(\mathrm{M})_{lit}$, as reported in the graph presented in Fig. 6.

As seen from Fig. 6, the agreement is correct only for **1** since its literature value $\Delta_p S^\circ(\mathrm{M})_{lit}$ is $15.8 \pm 7.2\,\mathrm{J\,mol^{-1}\,K^{-1}}$ while $\Delta_p S^\circ(\mathrm{M})_{iso}$ is equal to $14.7 \pm 1.9\,\mathrm{J\,mol^{-1}\,K^{-1}}$ (Table 2). It is an euphemism to said that the comparison is less satisfactorily for the bifunctional bases. For the diols **2**–**4**, the deviations observed between $\Delta_p S^\circ(\mathrm{M})_{iso}$ and $\Delta_p S^\circ(\mathrm{M})_{lit}$ is considerable, the former represents less than 20% of $\Delta_p S^\circ(\mathrm{M})_{lit}$. The situation is slightly less dramatic

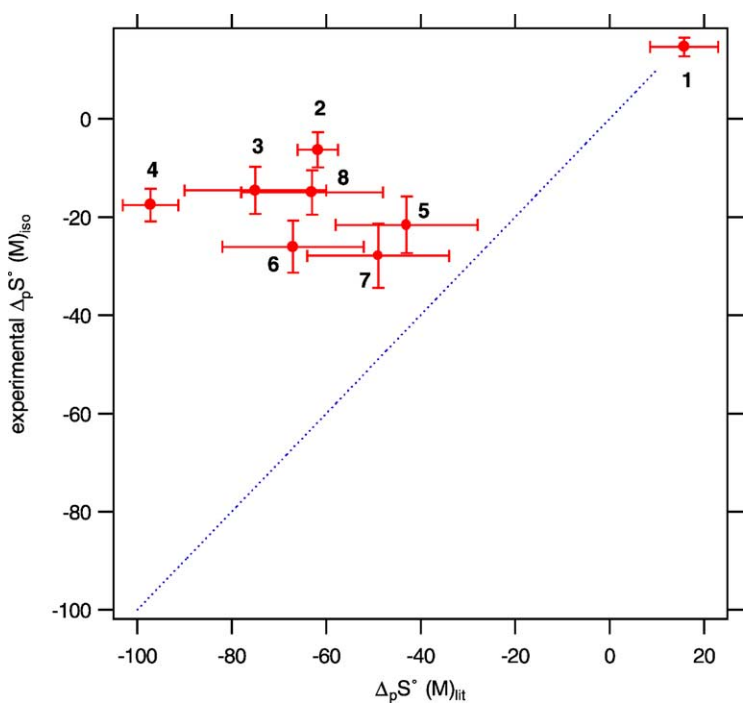

Fig. 6. Entropy difference $\Delta_p S^\circ(\mathrm{M})$ deduced from the isothermal point (Eq. (3c′)) compared to its literature value (ref. [12]).

for the two aminoalcohols **5**, **6**, and the diamines **7**, **8** since, for these four molecules, the experimental term $\Delta_p S^\circ(M)_{iso}$ represent a percentage situated between 25 and 60% of $\Delta_p S^\circ(M)_{lit}$. From these results, it is evident that the extended kinetic method does not provide a protonation entropy comparable to that given by the equilibrium method.

- The observed discrepancies may be interpreted by a couple of ways. One may either consider that Eqs. (3a′)–(3c′) (and thus Eqs. (2a′) and (2b′)) are not suitable for the determination of the protonation thermochemistry of bifunctional bases, or (and) that the PA, GB and $\Delta_p S^\circ$ values quoted in the literature are subjected to significant errors, particularly for the diols **2**–**4**. These points are briefly discussed below.

  The role of reverse activation enthalpy, $\Delta_R H^\ddagger$, or activation entropy, $\Delta S^\ddagger$, has been invoked to explain the difference between results obtained by the equilibrium method on the proton transfer reaction: $M + [B_iH]^+ \rightarrow [MHB_i]^+ \rightarrow [MH]^+ + B_i$, and by the kinetic method on the competitive dissociations of the proton bound dimer $[MHB_i]^+$ as depicted in Scheme 1. Although the same part of the corresponding potential energy surface is involved in both experiments,[1] differences arise from the internal energy content of the involved species. For example, $[MHB_i]^+$ is a reactive intermediate in the equilibrium experiments and a species successively thermalised in the ion source (CI or ESI experiments) and activated by collisions in the kinetic method experiments. However, these differences are expected to be taken into account by differences in the effective temperature *T*. By contrast, the sets of reactants and products are thermalised during equilibrium experiments thus allowing the determination of ΔG°, not $\Delta G^\ddagger$, from the equilibrium constant value. This latter point should be at the origin of results at variance from that obtained by the kinetic method and may be taken into account by using Eqs. (3a)–(3c) (or its precursor Eqs. (2a) and (2b)).

  The incidence of Eqs. (3a) and (3b) upon the proton affinity and gas phase basicity determinations is simply to shift $PA_{iso}(M)$ (and $GB_{iso}(M)$) by the $\Delta_R H^\ddagger$ term. The general comparison between $PA_{iso}(M)$ and $PA_{298}(M)$ presented in Fig. 5 may be taken as indicative of positive $\Delta_R H^\ddagger$ values. This is not unexpected in the present cases since a greater stabilisation should follow the formation of the products $B_i + [MH]^+$ by the strengthening of the internal hydrogen bond in $[MH]^+$ during its separation from B_i. As indicated above, $PA_{iso}(M)$ is close to $PA_{298}(M)$ within $\sim$10 kJ mol^{-1} for five of the molecules studied (**1** and **5**–**8**). This is almost comparable to the absolute experimental error on these quantities thus pointing to a limited participation of $\Delta_R H^\ddagger$ for these examples. By contrast, the diols **2**–**4** exhibit differences $PA_{298}(M)$–$PA_{iso}(M)$ in the range 20–30 kJ mol^{-1} which may be interpreted by the existence of a significant $\Delta_R H^\ddagger$, a firm conclusion however deserves further investigation.

  The discrepancies between the $\Delta_p S^\circ(M)$ values obtained by the kinetic method and from variable temperature equilibrium measurements is the second major observation. Eq. (3c) states that the entropy term accessible by the kinetic method is only the activation entropy difference $\Delta S^\ddagger$, thus the ΔS_{iso} values quoted in Table 2 corresponds in fact to $\Delta S^\ddagger$. As a whole, our results means that $\Delta S^\ddagger$ represents only 20–80% of the difference in entropy between $[MH]^+ + B_i$ and $M + [B_iH]^+$: the entropy loss is less pronounced when considering the transition structures than the products. Again, this would be not surprising if the constraints due to the internal hydrogen bond are less pronounced in the transition state than in the products $[MH]^+ + B_i$. These questions should be clarified by a careful examination of the structures involved, including the transition states for dissociation. Finally, another closely related view is to consider that the ΔS term determined by the kinetic method cannot

[1] This statement must be attenuated by the possibility of formation, for a given pair of molecules M and B, of protonated structures different from a proton bound dimer. Other ion–neutral complexes or covalent species may exist as stable structures and their interconnection on the potential energy surface and their possible sampling during the kinetic experiments should be considered.

be equated to a true thermodynamic entropy difference as recently suggested [2d,2f,4c,6]. Rather, in a microcanonical treatment of the kinetic method, the measured ΔS should be related to the ratio of the sum of rovibrational states of the transitions states of both dissociation channels [2d].

4. Conclusion

The first conclusion that emerges from the present study is that the application of the kinetic method to polydentate bases should be imperatively conducted in the frame of the "extended kinetic method" or the inherently equivalent "isothermal point" analysis. The simple treatment which make use of the intercept of the $\ln([MH]^+/[B_iH]^+)$ versus $PA(B_i)$ (or $GB(B_i)$) plot with the *x*-axis leads to erroneous results. As a consequence, a careful re-examination of all the literature data obtained during the years by the kinetic method for polydentate molecules is hopefully.

The present results suggest that the co-ordinates of the isothermal point in the $\ln([MH]^+/[B_iH]^+)$ versus $PA(B_i)$ plot may be only used to deduce a lower bound for the proton affinity of a polyfunctional base M. The equality $PA_{iso}(M) = PA'_{iso}(M) = PA_{298}(M)$ (Eqs. (3a′) and (3a″)) holds exclusively for the acetone molecule **1**. The reasons for these discrepancies, particularly for the diols **2**–**4**, should be clarified by new experiments, or (and) by new computations.

The experimental entropy term ΔS°_{iso} seems to be qualitatively related to the difference $\Delta S^\circ = S^\circ([MH]^+ + B_i) - S^\circ(M + [B_iH]^+)$, but for all the bidentate bases examined, ΔS°_{iso} appears to be significantly less than ΔS° when this latter is estimated using protonation entropy obtained by variable temperature equilibrium constant measurement. These observations are in keeping with other which lead to the proposal that apparent entropy values obtained from the extended kinetic method are not valid thermodynamic entropies [2d,2f,4c,6]. A more correct approach to the kinetic method is to relate y_i to energetic characteristics of the dissociations by a complete calculation of the product ions abundances via a proper statistical rate constant evaluation. This procedure, first introduced by Nielsen and Bojesen [19] and recently advocated by Brauman and co-workers [20], Laskin et al. [2f,2g] and Ervin [2d], should be developed in order to precise the relationship between the observable and the thermodynamic quantities.

Appendix A

Tables A.1–A.8 contain the various data used in the present study for each molecule M = **1**–**8**: the natural logarithm of the ratio of peaks height $[MH]^+/[B_iH]^+$ and the tabulated [12] proton affinities, gas phase basicities and protonation entropies of the reference bases B_i.

The corresponding representative plots $y_i = \ln([MH]^+/[B_iH]^+)$ versus $PA(B_i)$ (in $kJ\,mol^{-1}$) are presented in Figs. A.1–A.8 for molecules M = **1**–**8**, respectively. The equations of the linear fits obtained at E_{cm} = 0, 2 and 4 eV are displayed together with the regression coefficient (Pr), the *x* intercept (PAeff), the isothermal proton affinity PA_{iso} (PAiso) and the isothermal protonation entropy ΔS°_{iso} (DSiso). The uncertainty on the $y_i = \ln([MH]^+/[B_iH]^+)$ values are generally less than ±0.4, thus error bars of ±0.4 are indicated on the y_i values in Figs. A.1–A.8.

The uncertainty given in Table 1 on the measured proton affinity and gas phase basicity are standard deviations. It is worthwhile to emphasise that it represents only a lower limit on the expected precision, which probably lies in the $5\,kJ\,mol^{-1}$ range. Other factors should obviously be considered, first of all the precision on the experimental y_i values and the tabulated $PA(B_i)$ and $GB(B_i)$ and, second, the number and the choice of the bases B_i. Our first observation is that PA(M) and GB(M) values obtained by a linear curve fitting procedure using either a weighting of y_i and $PA(B_i)$ (with errors of ±0.4 and $\pm 4.0\,kJ\,mol^{-1}$, respectively), or not, are essentially the same. However, the incidence of a wrong PA or GB value is crucial. Accordingly, we generally observed that changing one $PA(B_i)$ by $4\,kJ\,mol^{-1}$ produces a shift of ca.

2 kJ mol^{-1} in the estimate of PA_{iso}. However, this unpredictable effect may be at the origin of larger deviations. An illustration is offered by the comparison of the PA_{iso} values reported for diamines **7** and **8** in refs. [4d,6] which differ by 6 and 22 kJ mol^{-1}, respectively because of a different choice of $PA(B_i)$ and $GB(B_i)$ values for several reference bases B_i. Another important point to consider is the number and the choice of the selected bases. This may be illustrated again by the cases of diamines **7** and **8**. Wang et al. [2c] and Hahn and Wesdemiotis [4f] obtained recently for **8**, PA_{iso} values as different as 1010 and 993 kJ mol^{-1}, respectively, by using only three points in the linear plots. In the same laboratory, PA_{iso} values of 974.5 and 980.5 kJ mol^{-1} were obtained for 1,3-diaminobutane (**7**), using again two sets of three points [2c]. Finally, we note also that the PA_{iso} value is better determined if the correlation lines are defined by experimental points situated in both sides of the intercept. In the present study, we tentatively limit such difficulties by using a set of five to nine reference bases B_i in order to obtain a meaningful correlation line. As seen in Figs. A.1–A.8, in most of the cases, the regression coefficient is better than, or close to 0.99.

Table A.1
Thermochemical data for reference bases B_i and natural logarithm of the experimental peak intensities ratio, $y_i = \ln([MH]^+/[B_iH]^+)$; M = acetone (**1**)

B_i	$GB(B_i)$[a]	$PA(B_i)$[a]	$\Delta_pS^\circ(B_i)$[a]	y_i		
				E_{cm}[b] = 0 eV	E_{cm}[b] = 2 eV	E_{cm}[b] = 4 eV
n-C_4H_9CN	771.7	802.4	6	4.71	3.81	3.09
i-C_3H_7CN	772.8	803.6	6	4.33	3.64	2.71
t-C_4H_9CN	780.2	810.9	6	1.82	1.72	1.63
C_6H_5CN	780.9	811.5	6	1.61	1.61	1.61
$CH_3CO_2CH_3$	790.7	821.6	5	−2.34	−1.82	−1.25
Cyclopentanone	794.0	823.7	9	−3.45	−2.44	−1.38
THF[c]	794.7	822.1	17	−4.69	−3.69	−3.00

[a] From the compilation by Hunter and Lias [12]. Gas phase basicity (GB) and proton affinity (PA) in kJ mol^{-1}. Protonation entropy as defined by: $\Delta_pS^\circ(B_i) = S^\circ([B_iH]^+) - S^\circ(B_i)$ (in J mol^{-1} K^{-1}).

[b] Centre of mass collision energy in eV.

[c] Base used exclusively for the $y_i' = y_i + \Delta_pS^\circ(B_i)/R$ vs. $PA(B_i)$ correlation (see text) because of its large Δ_pS° value compared to the mean value of the other six reference bases (6.3 J mol^{-1} K^{-1}).

Table A.2
Thermochemical data for reference bases B_i and natural logarithm of the experimental peak intensities ratio, $y_i = \ln([MH]^+/[B_iH]^+)$; M = 1,3-propanediol (**2**)

B_i	$GB(B_i)$[a]	$PA(B_i)$[a]	$\Delta_pS^\circ(B_i)$[a]	y_i		
				E_{cm}[b] = 0 eV	E_{cm}[b] = 2 eV	E_{cm}[b] = 4 eV
t-C_4H_9CN	780.2	810.9	6	8.11	6.32	4.54
Cyclo-$C_6H_{11}N$	784.4	815.0	6	7.84	6.20	4.55
$CH_3CO_2CH_3$	790.7	821.6	5	5.20	3.56	1.92
3-Pentanone	807.0	836.8	9	4.24	2.59	0.95
4-Heptanone	815.3	845.0	9	1.03	0.36	−0.32
Methyl-cyclopropyl ketone	823.0	854.9	2	−0.58	−0.77	−0.97
$(Cyclopropyl)_2CO$	850.6	880.4	9	−6.99	−5.61	−4.24

[a] From the compilation by Hunter and Lias [12]. Gas phase basicity (GB) and proton affinity (PA) in kJ mol^{-1}. Protonation entropy as defined by: $\Delta_pS^\circ(B_i) = S^\circ([B_iH]^+) - S^\circ(B_i)$ (in J mol^{-1} K^{-1}).

[b] Centre of mass collision energy in eV.

Table A.3
Thermochemical data for reference bases B_i and natural logarithm of the experimental peak intensities ratio, $y_i = \ln([MH]^+/[B_iH]^+)$; M = glycerol (**3**)

B_i	$GB(B_i)$[a]	$PA(B_i)$[a]	$\Delta_pS^\circ(B_i)$[a]	y_i		
				E_{cm}[b] = 0 eV	E_{cm}[b] = 2 eV	E_{cm}[b] = 4 eV
2-Pentanone	800.9	832.7	2	2.07	1.28	0.48
3-Methylbutanone	804.4	836.3	2	1.66	0.65	−0.36
3-Pentanone	807.0	836.8	9	1.52	0.47	−0.58
t-$C_4H_9COCH_3$	810.9	842.8	2	−0.19	−0.72	−1.24
Cyclohexanone	811.2	841.0	9	−0.09	−0.55	−1.00
t-$C_4H_9OCH_3$	812.4	841.6	11	−0.43	−0.51	−0.60
Cycloheptanone	815.9	845.6	9	−1.68	−1.78	−1.88
Cyclooctanone	819.6	849.4	9	−3.13	−3.16	−3.19

[a] From the compilation by Hunter and Lias [12]. Gas phase basicity (GB) and proton affinity (PA) in kJ mol^{-1}. Protonation entropy as defined by: $\Delta_pS^\circ(B_i) = S^\circ([B_iH]^+) - S^\circ(B_i)$ (in J mol^{-1} K^{-1}).
[b] Centre of mass collision energy in eV.

Table A.4
Thermochemical data for reference bases B_i and natural logarithm of the experimental peak intensities ratio, $y_i = \ln([MH]^+/[B_iH]^+)$; M = 1,4-butanediol (**4**)

B_i	$GB(B_i)$[a]	$PA(B_i)$[a]	$\Delta_pS^\circ(B_i)$[a]	y_i		
				E_{cm}[b] = 0 eV	E_{cm}[b] = 2 eV	E_{cm}[b] = 4 eV
Methyl-cyclopropyl ketone	823.0	854.9	2	4.95	3.52	2.08
3-Pentene-2-one	832.5	864.3	2	2.55	1.96	1.38
4-Methyl-3-pentene-2-one	846.9	878.7	2	−0.22	−0.92	−1.62
DMSO	853.7	884.4	5.8	−2.16	−2.79	−3.60
N,*N*-Dimethyl formamide	856.6	887.5	5	−2.28	−2.95	−3.62
N-Ethyl acetamide	867.0	898.0	5	−6.1	−5.29	−4.48
2-Chloropyridine	869.0	900.9	2	−8.57	−6.48	−4.40
2,4-Pentanedione[c]	836.8	873.5	−14	2.69	1.44	0.20
2,5-Hexanedione[c]	851.8	892.0	−26	−1.67	−1.17	−0.68

[a] From the compilation by Hunter and Lias [12]. Gas phase basicity (GB) and proton affinity (PA) in kJ mol^{-1}. Protonation entropy as defined by: $\Delta_pS^\circ(B_i) = S^\circ([B_iH]^+) - S^\circ(B_i)$ (in J mol^{-1} K^{-1}).
[b] Centre of mass collision energy in eV.
[c] Base used exclusively for the $y'_i = y_i + \Delta_pS^\circ(B_i)/R$ vs. $PA(B_i)$ correlation (see text).

Table A.5
Thermochemical data for reference bases B_i and natural logarithm of the experimental peak intensities ratio, $y_i = \ln([MH]^+/[B_iH]^+)$; M = 1,3-propanolamine (**5**)

B_i	$GB(B_i)$[a]	$PA(B_i)$[a]	$\Delta_pS^\circ(B_i)$[a]	y_i		
				E_{cm}[b] = 0 eV	E_{cm}[b] = 2 eV	E_{cm}[b] = 4 eV
Pyridine	898.1	930.0	2	4.29	3.11	1.93
t-Butyl amine	899.9	934.1	−6	2.30	1.62	0.93
4-Methyl pyridine	915.3	947.2	2	0.19	−0.12	−0.43
Pyrrolidine	915.3	948.3	−2	−0.66	−1.42	−2.17
Diethyl amine	919.4	952.4	−1.9	−1.74	−2.17	−2.59
i-Propylmethyl amine	919.4	952.4	−8	−1.15	−1.48	−1.80
2,5-Dimethyl pyridine	926.9	958.8	2	−4.94	−3.90	−2.85
Dipropyl amine	929.3	962.3	−1.9	−4.66	−4.36	−4.05

[a] From the compilation by Hunter and Lias [12]. Gas phase basicity (GB) and proton affinity (PA) in kJ mol^{-1}. Protonation entropy as defined by: $\Delta_pS^\circ(B_i) = S^\circ([B_iH]^+) - S^\circ(B_i)$ (in J mol^{-1} K^{-1}).
[b] Centre of mass collision energy in eV.

Table A.6
Thermochemical data for reference bases B_i and natural logarithm of the experimental peak intensities ratio, $y_i = \ln([MH]^+/[B_iH]^+)$; M = 1,4-butanolamine (**6**)

B_i	GB(B_i)[a]	PA(B_i)[a]	$\Delta_pS^\circ(B_i)$[a]	y_i		
				E_{cm}[b] = 0 eV	E_{cm}[b] = 2 eV	E_{cm}[b] = 4 eV
4-Methyl pyridine	915.3	947.2	2	3.74	2.23	0.71
Pyrrolidine	915.3	948.3	−2	3.46	1.12	−1.22
i-Propylmethyl amine	919.4	952.4	−8	2.87	0.98	−0.92
2,5-Dimethyl pyridine	926.9	958.8	2	0.35	−0.47	−1.30
Di-*n*-propyl amine	929.3	962.3	−1.9	−0.73	−1.60	−2.47
Di-*i*-propyl amine	938.6	971.9	−1.9	−2.27	−2.74	−3.22
Triethyl amine	951.0	981.8	5.6	−5.43	−5.57	−5.71
2,2,6,6-Tetramethyl piperidine	953.9	987.0	−1.9	−8.30	−6.35	−4.40

[a] From the compilation by Hunter and Lias [12]. Gas phase basicity (GB) and proton affinity (PA) in kJ mol^{-1}. Protonation entropy as defined by: $\Delta_pS^\circ(B_i) = S^\circ([B_iH]^+) - S^\circ(B_i)$ (in J mol^{-1} K^{-1}).
[b] Centre of mass collision energy in eV.

Table A.7
Thermochemical data for reference bases B_i and natural logarithm of the experimental peak intensities ratio, $y_i = \ln([MH]^+/[B_iH]^+)$; M = 1,3-propanediamine (**7**)

B_i	GB(B_i)[a]	PA(B_i)[a]	$\Delta_pS^\circ(B_i)$[a]	y_i		
				E_{cm}[b] = 0 eV	E_{cm}[b] = 2 eV	E_{cm}[b] = 4 eV
Dipropyl amine	929.3	962.3	−1.9	3.24	1.50	−0.20
1-Methylpyrrolidine	934.8	965.6	5.6	1.89	−0.25	−1.46
1-Methylpiperidine	940.1	971.1	5.6	0.26	−0.71	−1.67
Diethylmethyl amine	940.0	971.0	5.6	−0.29	−1.35	−2.47
Triethyl amine	951.0	981.8	5.6	−4.44	−4.32	−4.19
2,2,6,6-Tetramethyl piperidine	953.9	987.0	−1.9	−5.49	−4.90	−4.31

[a] From the compilation by Hunter and Lias [12]. Gas phase basicity (GB) and proton affinity (PA) in kJ mol^{-1}. Protonation entropy as defined by: $\Delta_pS^\circ(B_i) = S^\circ([B_iH]^+) - S^\circ(B_i)$ (in J mol^{-1} K^{-1}).
[b] Centre of mass collision energy in eV.

Table A.8
Thermochemical data for reference bases B_i and natural logarithm of the experimental peak intensities ratio, $y_i = \ln([MH]^+/[B_iH]^+)$; M = 1,4-butanediamine (**8**)

B_i	GB(B_i)[a]	PA(B_i)[a]	$\Delta_pS^\circ(B_i)$[a]	y_i		
				E_{cm}[b] = 0 eV	E_{cm}[b] = 2 eV	E_{cm}[b] = 4 eV
Di-*n*-propyl amine	929.3	962.3	−1.9	4.75	2.87	0.97
1-Methylpyrrolidine	934.8	965.6	5.6	3.81	2.03	0.27
Diethylmethyl amine	940.0	971.0	5.6	3.29	1.47	−0.36
Tripropyl amine	960.1	991.0	5.6	−2.42	−2.28	−2.14
Tri-*n*-butyl amine	967.6	998.5	5.6	−3.84	−3.41	−3.00

[a] From the compilation by Hunter and Lias [12]. Gas phase basicity (GB) and proton affinity (PA) in kJ mol^{-1}. Protonation entropy as defined by: $\Delta_pS^\circ(B_i) = S^\circ([B_iH]^+) - S^\circ(B_i)$ (in J mol^{-1} K^{-1}).
[b] Centre of mass collision energy in eV.

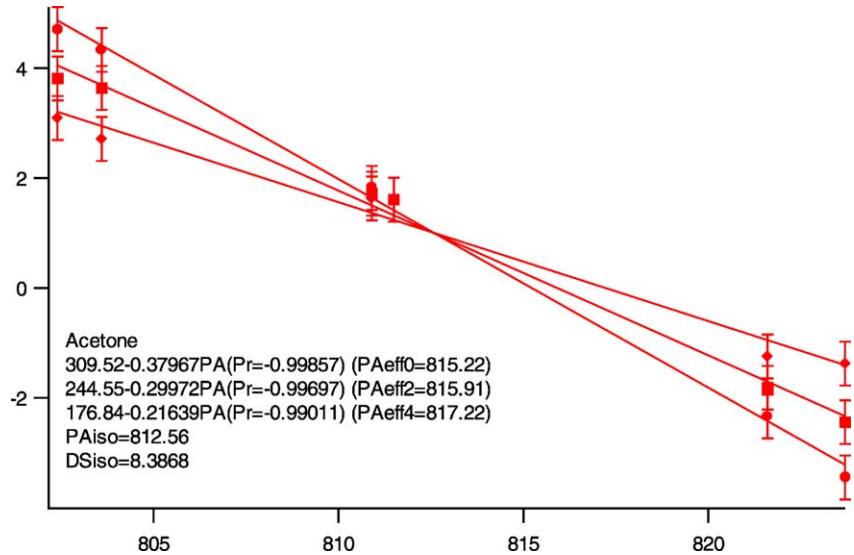

Fig. A.1. Plot of $y_i = \ln([MH]^+/[B_iH]^+)$ vs. PA(B_i) for M = acetone (**1**), and correlation lines at $E_{cm} = 0$, 2 and 4 eV.

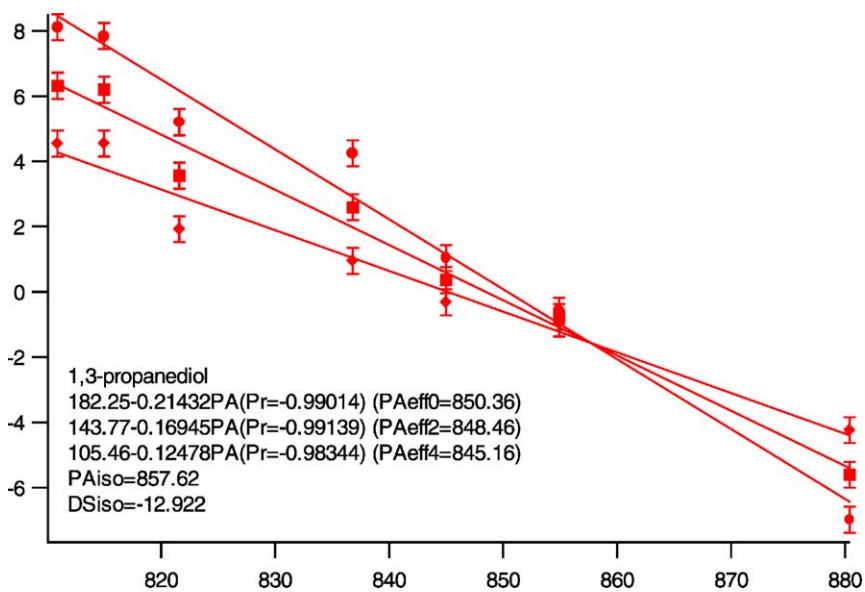

Fig. A.2. Plot of $y_i = \ln([MH]^+/[B_iH]^+)$ vs. PA(B_i) for M = 1,3-propanediol (**2**), and correlation lines at $E_{cm} = 0$, 2 and 4 eV.

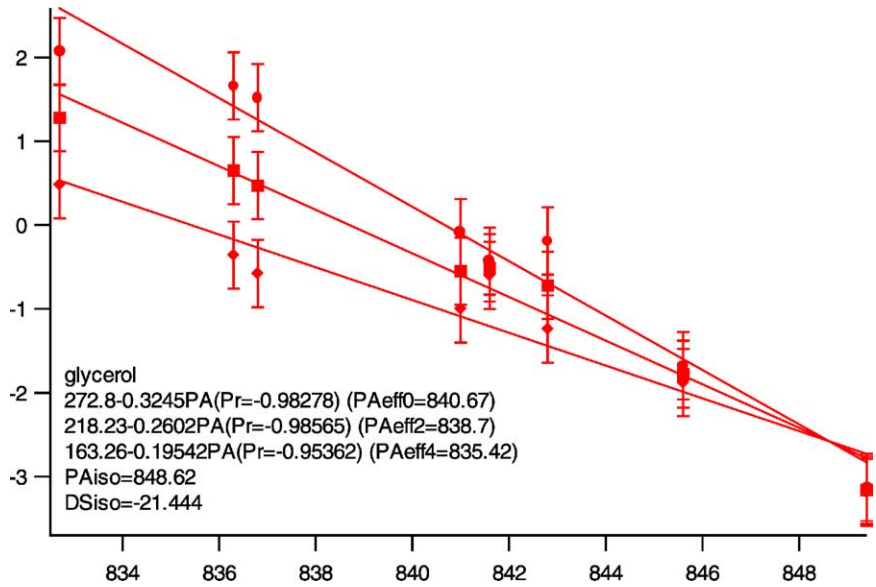

Fig. A.3. Plot of $y_i = \ln([MH]^+/[B_iH]^+)$ vs. $PA(B_i)$ for M = glycerol (**3**), and correlation lines at $E_{cm} = 0$, 2 and 4 eV.

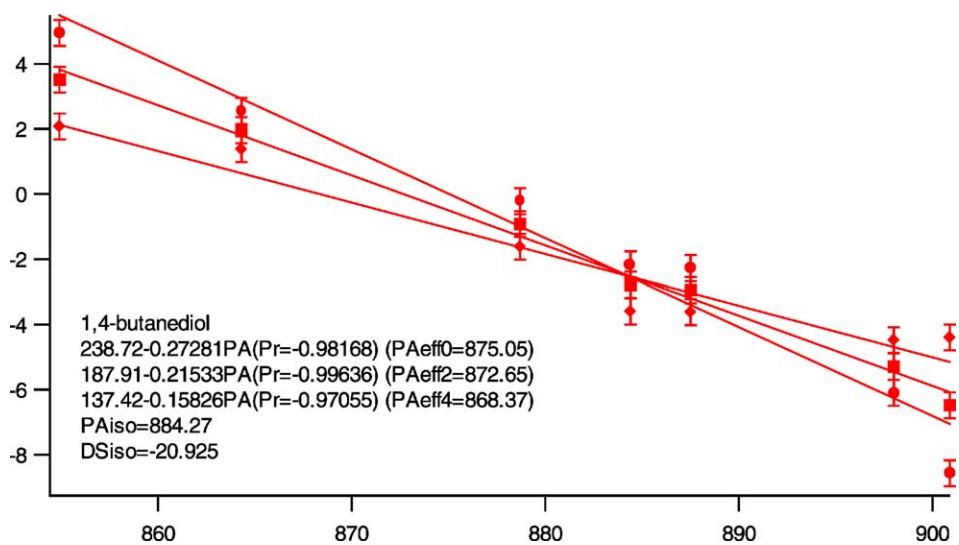

Fig. A.4. Plot of $y_i = \ln([MH]^+/[B_iH]^+)$ vs. $PA(B_i)$ for M = 1,4-butanediol (**4**), and correlation lines at $E_{cm} = 0$, 2 and 4 eV.

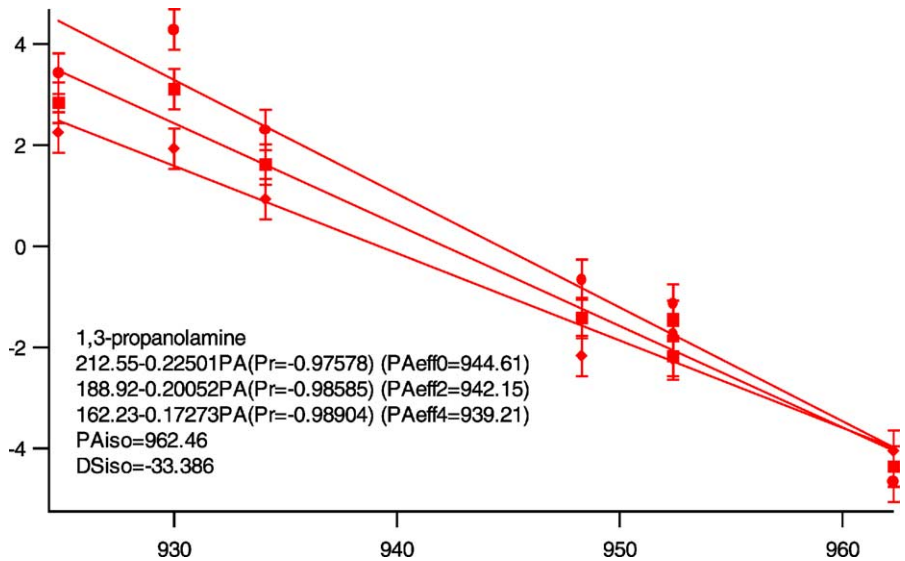

Fig. A.5. Plot of $y_i = \ln([MH]^+/[B_iH]^+)$ vs. $PA(B_i)$ for M = 1,3-propanolamine (**5**), and correlation lines at $E_{cm} = 0$, 2 and 4 eV.

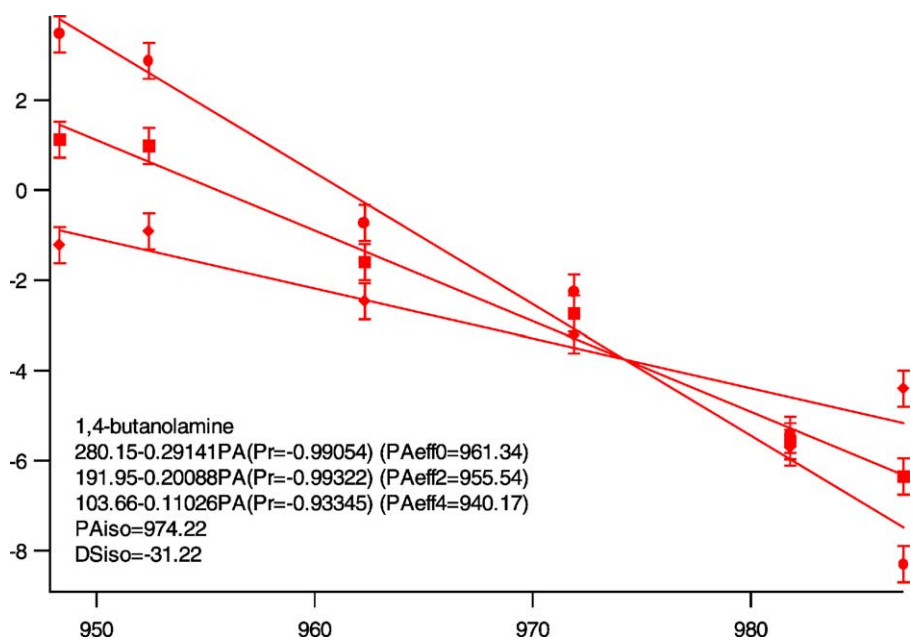

Fig. A.6. Plot of $y_i = \ln([MH]^+/[B_iH]^+)$ vs. $PA(B_i)$ for M = 1,4-butanolamine (**6**), and correlation lines at $E_{cm} = 0$, 2 and 4 eV.

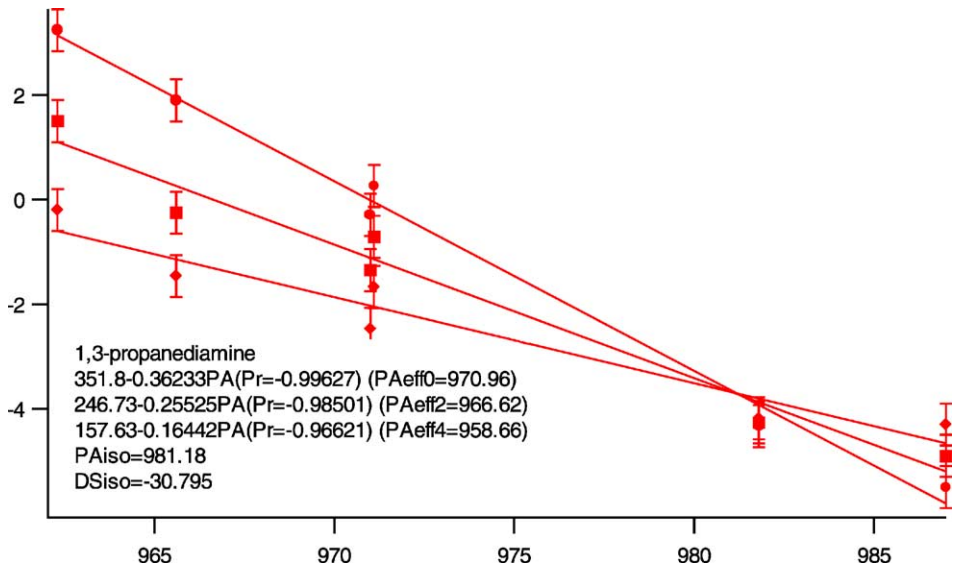

Fig. A.7. Plot of $y_i = \ln([MH]^+/[B_iH]^+)$ vs. PA(B_i) for M = 1,3-propanediamine (**7**), and correlation lines at $E_{cm} = 0$, 2 and 4 eV.

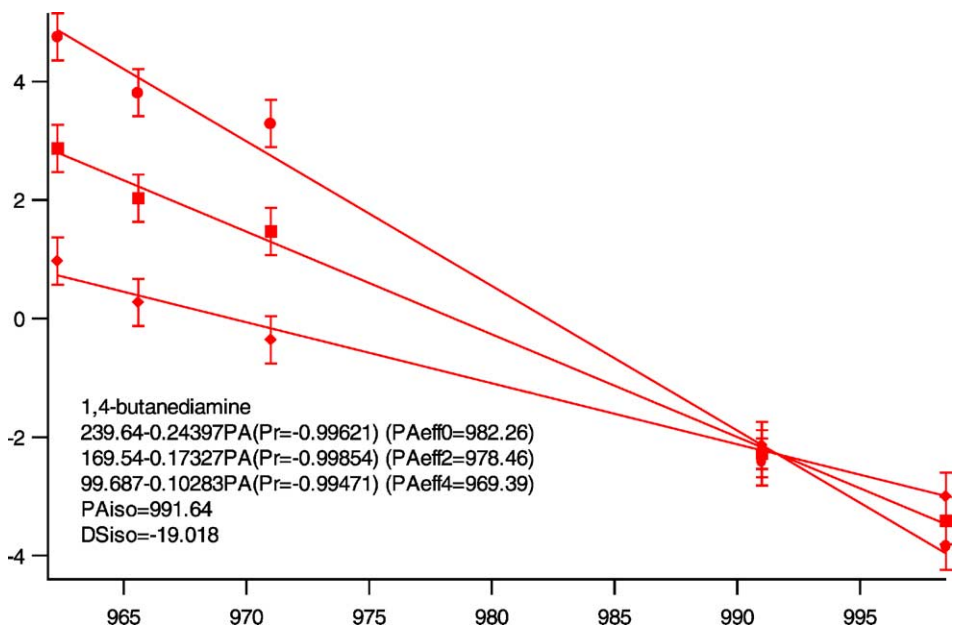

Fig. A.8. Plot of $y_i = \ln([MH]^+/[B_iH]^+)$ vs. PA(B_i) for M = 1,4-butanediamine (**8**), and correlation lines at $E_{cm} = 0$, 2 and 4 eV.

References

[1] (a) R.G. Cooks, J.S. Patrick, T. Kotaho, S.A. McLuckey, Mass Spectrom. Rev. 13 (1994) 287;
(b) R.G. Cooks, P.S.H. Wong, Account Chem. Res. 31 (1998) 379;
(c) R.G. Cooks, J.T. Koskinen, P.D. Thomas, J. Mass Spectrom. 34 (1999) 85;
(d) K. Ervin, Chem. Rev. 101 (2001) 391;
(e) J.F. Gal, P.C. Maria, E. Raczynska, J. Mass Spectrom. 36 (2001) 699.

[2] (a) P.B. Armentrout, J. Mass Spectrom. 34 (1999) 74;
(b) P.B. Armentrout, J. Am. Soc. Mass Spectrom. 11 (2000) 371;
(c) Z. Wang, I.K. Chu, C.F. Rodriquez, A.C. Hopkinson, K.W.M. Siu, J. Phys. Chem. 103 (1999) 8700;
(d) K.M. Ervin, J. Am. Soc. Mass Spectrom. 13 (2002) 435;
(e) X. Zheng, R.G. Cooks, J. Phys. Chem. A 106 (2002) 9939;
(f) J. Laskin, J.H. Futrell, J. Phys. Chem. 104 (2000) 8829;
(g) J.J. Hache, J. Laskin, J.H. Futrell, J. Phys. Chem. 106 (2002) 12051.

[3] (a) X. Cheng, Z. Wu, C. Fenselau, J. Am. Chem. Soc. 115 (1993) 4844;
(b) Z. Wu, C. Fenselau, Rapid Commun. Mass Spectrom. 8 (1994) 777;
(c) B.A. Cerda, C. Wesdemiotis, J. Am. Chem. Soc. 118 (1996) 11884;
(d) B.A. Cerda, S. Hoyau, G. Ohanessian, C. Wesdemiotis, J. Am. Chem. Soc. 120 (1998) 2437;
(e) B.A. Cerda, C. Wesdemiotis, Int. J. Mass Spectrom. 185–187 (1999) 107;
(f) M.J. Nold, B.A. Cerda, C. Wesdemiotis, J. Am. Soc. Mass Spectrom. 10 (1999) 1;
(g) M. Witt, H.-F. Grutzmacher, Eur. J. Mass Spectrom. 6 (2000) 97;
(h) P.G. Wenthold, J. Am. Soc. Mass Spectrom. 11 (2000) 601;
(i) H.A. Lardin, R.R. Squires, P.G. Wenthold, J. Mass Spectrom. 36 (2001) 607;
(j) L. Di Donna, A. Napoli, G. Sindona, Int. J. Mass Spectrom. 210/211 (2001) 165;
(k) T.I. Williams, J.W. Denault, R.G. Cooks, Int. J. Mass Spectrom. 210/211 (2001) 133;
(l) A.F. Kuntz, A.W. Boynton, G.A. David, K.E. Colyer, J.C. Poutsma, J. Am. Soc. Mass Spectrom. 13 (2002) 72.

[4] (a) J.L. Holmes, C. Aubry, P.M. Mayer, J. Phys. Chem. A 103 (1999) 705;
(b) J. Cao, J.L. Holmes, Eur. Mass Spectrom. 5 (1999) 19;
(c) J. Cao, C. Aubry, J.L. Holmes, J. Phys. Chem. A 104 (2000) 10045;
(d) J. Cao, J.L. Holmes, Int. J. Mass Spectrom. 195/196 (2000) 525;
(e) N. Morlender-Vais, J.L. Holmes, Int. J. Mass Spectrom. 210/211 (2001) 147;
(f) I.-S. Hahn, C. Wesdemiotis, Int. Mass Spectrom. 222 (2003) 465.

[5] P. D Thomas, R.G. Cooks, K. Vekey, L. Drahos, C. Wesdemiotis, J. Phys. Chem. A 104 (2000) 1359.

[6] G. Bouchoux, F. Djazi, F. Gaillard, D. Vierezet, Int. J. Mass Spectrom, in press.

[7] Q.F. Chen, J.A. Stone, J. Phys. Chem. 99 (1995) 1442.

[8] J.A. Sunner, R. Kulatunga, P. Kebarle, Anal. Chem. 58 (1986) 1312.

[9] M. Mautner, P. Hamlet, E.P. Hunter, F.H. Field, J. Am. Chem. Soc. 102 (1980) 6393.

[10] D.H. Aue, H.M. Webb, M.T. Bowers, J. Am. Chem. Soc. 95 (1973) 2699.

[11] R. Yamdagni, P. Kebarle, J. Am. Chem. Soc. 95 (1973) 3504.

[12] E.P. Hunter, S.G. Lias, J. Phys. Chem. Ref. Data 413 (1998) 27;
NIST Chemistry Webbook, Standard Reference Database 69, 1998.

[13] G. Bouchoux, N. Choret, F. Berruyer-Penaud, R. Flammang, Int. J. Mass Spectrom. 217 (2002) 195.

[14] G. Bouchoux, N. Choret, F. Berruyer-Penaud, J. Phys. Chem. A 105 (2001) 3589.

[15] J.E. Szulejko, T.B. McMahon, Int. J. Mass Spectrom. Ion Process. 109 (1991) 279.

[16] J.E. Szulejko, T.B. McMahon, J. Am. Chem. Soc. 115 (1993) 7839.

[17] M. Mautner, L.W. Sieck, J. Am. Chem. Soc. 113 (1991) 4448.

[18] L.W. Sieck, J. Phys. Chem. A 101 (1997) 8140.

[19] S.B. Nielsen, G. Bojesen, Eur. J. Mass Spectrom. 1 (1995) 423.

[20] S.L. Craig, M. Zhong, B. Choo, J.I. Brauman, J. Phys. Chem. A 101 (1997) 19.